Neurobiology of Disease 207 (2025) 106849

Contents lists available at ScienceDirect

Neurobiology of Disease

journal homepage: www.elsevier.com/locate/ynbdi

Dysregulated balance of D- and L-amino acids modulating glutamatergic neurotransmission in severe spinal muscular atrophy

Amber Hassan [a,b,1], Raffaella di Vito [a,c,1], Tommaso Nuzzo [a,c,1], Matteo Vidali [d], Maria Jose Carlini [e], Shubhi Yadav [e], Hua Yang [e], Adele D'Amico [f], Xhesika Kolici [g,h], Valeria Valsecchi [g], Chiara Panicucci [i], Giuseppe Pignataro [g], Claudio Bruno [i,j], Enrico Bertini [f], Francesco Errico [a,k], Livio Pellizzoni [e,l,m], Alessandro Usiello [a,b,c,*]

[a] Laboratory of Translational Neuroscience, Ceinge Biotecnologie Avanzate "Franco Salvatore", 80145 Naples, Italy
[b] European School of Molecular medicine, University of Milan, Milan, Italy
[c] Department of Environmental, Biological and Pharmaceutical Science and Technologies, Università degli Studi della Campania "Luigi Vanvitelli", 81100 Caserta, Italy
[d] Clinical Pathology Unit, Fondazione IRCCS Ca' Granda Ospedale Maggiore Policlinico, Milano, Italy
[e] Department of Neurology, Columbia University, New York, NY, USA
[f] Unit of Neuromuscular and Neurodegenerative Disorders, Dept. Neurosciences, Bambino Gesu' Children's Hospital IRCCS, Roma, Italy
[g] Division of Pharmacology, Department of Neuroscience, Reproductive and Dentistry Sciences, School of Medicine, University of Naples "Federico II", 80131 Naples, Italy
[h] School of Advanced Studies, Centre for Neuroscience, University of Camerino, Italy
[i] Center of Translational and Experimental Myology, IRCCS Istituto Giannina Gaslini, Genova, Italy
[j] Department of Neuroscience, Rehabilitation, Ophthalmology, Genetics, Maternal, and Child Health - DINOGMI, University of Genova, Genova, Italy
[k] Department of Agricultural Sciences, University of Naples "Federico II", Portici 80055, Italy
[l] Center for Motor Neuron Biology and Disease, Columbia University, New York, NY, USA
[m] Department of Pathology and Cell Biology, Columbia University, New York, NY, USA

ARTICLE INFO

Keywords:
Spinal muscular atrophy
Cerebrospinal fluid
Nusinersen
Central nervous system
Glutamatergic neurotransmission
NMDA receptors
D-serine

ABSTRACT

Spinal muscular atrophy (SMA) is a neuromuscular disorder caused by reduced expression of the survival motor neuron (SMN) protein. In addition to motor neuron survival, SMN deficiency affects the integrity and function of afferent synapses that provide glutamatergic excitatory drive essential for motor neuron firing and muscle contraction. However, it is unknown whether deficits in the metabolism of excitatory amino acids and their precursors contribute to neuronal dysfunction in SMA. To address this issue, we measured the levels of the main neuroactive D- and L-amino acids acting on glutamatergic receptors in the central nervous system of SMNΔ7 mice as well as the cerebrospinal fluid (CSF) of SMA patients of varying severity before and after treatment with the SMN-inducing drug Nusinersen. Our findings reveal that SMN deficiency is associated with disruption of glutamate and serine metabolism in the CSF of severe SMA patients, including decreased concentration of L-glutamate, which is partially corrected by Nusinersen therapy. Moreover, we identify dysregulated L-glutamine/L-glutamate ratio as a shared neurochemical signature of altered glutamatergic synapse metabolism that implicates neuron-astrocyte dysfunction in both severe SMA patients and mouse models. Lastly, consistent with hypo-glutamatergic neurotransmission in SMA, we show that daily supplementation with the NMDA receptor co-agonist D-serine improves neurological deficits in SMNΔ7 mice. Altogether, these findings provide direct evidence for central dysregulation of D- and L-amino acid metabolism linked to glutamatergic neurotransmission in severe SMA and have potential implications for treating this neurological disorder.

Abbreviations: ANCOVA, analysis of covariance; ANOVA, analysis of variance; CHOP-INTEND, Children's Hospital of Philadelphia infant test of neuromuscular disorders; BMI, body mass index; CNS, central nervous system; CSF, cerebrospinal fluid; D-Asp, D-aspartate; D-Ser, D-serine; HFMSE, Hammersmith functional motor scale-expanded; HPLC, high-performance liquid chromatography; IP, intraperitoneal; IQR, interquartile range; L-Asp, L-aspartate; L-Gln, L-glutamine; L-Glu, L-glutamate; L-Ser, L-serine; mGluR, metabotropic glutamate receptor; NIV, non-invasive ventilation; NMDA, *N*-methyl D-aspartate; NMDAR, NMDA receptor; SMA, spinal muscular atrophy; SMN, survival motor neuron; TCA, trichloroacetic acid; WT, wild-type..

* Corresponding author at: Department of Environmental, Biological and Pharmaceutical Sciences and Technologies, University of Campania "Luigi Vanvitelli", Via A. Vivaldi, 43, 81100 Caserta, Italy.
E-mail address: usiello@ceinge.unina.it (A. Usiello).
[1] These authors contributed equally to this work.

https://doi.org/10.1016/j.nbd.2025.106849
Received 6 November 2024; Received in revised form 6 February 2025; Accepted 17 February 2025
Available online 24 February 2025

1. Introduction

Spinal muscular atrophy (SMA) is the most common genetic cause of infant mortality and is characterized by the progressive degeneration of spinal motor neurons and skeletal muscle atrophy (Kong et al., 2021; Nishio et al., 2023; Wirth et al., 2020), with increasing evidence of multiorgan pathology (Mercuri et al., 2020; Nishio et al., 2023). SMA is caused by homozygous mutations in the *Survival Motor Neuron 1 (SMN1)* gene (Lefebvre et al., 1995), while the paralogue gene *SMN2* - which is present in variable copy numbers - can only partially compensate for *SMN1* loss due to a single nucleotide change affecting its pre-mRNA splicing (Tisdale and Pellizzoni, 2015). SMA patients are classified into five main clinical groups (the classical type 1, 2 and 3, congenital type 0, and adult onset type 4) based on the age of onset and severity of the disease, which inversely correlate with the number of *SMN2* copies and the SMN protein levels (Wirth et al., 2020).

Three different therapeutic approaches aimed at increasing SMN expression through splicing modulation or viral-mediated gene replacement have been approved for the treatment of SMA (Mercuri et al., 2020). Among these, Nusinersen (Spinraza®) - the first FDA-approved drug for the treatment of SMA (Finkel et al., 2017) - is an antisense oligonucleotide administered intrathecally that corrects the splicing of *SMN2* pre-mRNA, increasing the concentration of functional SMN protein (Mercuri et al., 2020; Tisdale and Pellizzoni, 2015; Wirth, 2021). Clinical data show that Nusinersen induces remarkable improvement of motor function in SMA patients, especially when treated early (Li et al., 2023). Despite significant advances in SMA therapy, however, the current consensus is that neither Nusinersen nor other treatments can cure the disease (Mercuri et al., 2020; Ravi et al., 2021; Wirth, 2021). In particular, there are still unmet needs to address the incomplete correction of disease symptoms and the variability in clinical response to treatment. One of the major limitations is the absence of validated targets whose modulation could enhance the clinical benefit of SMN-inducing drugs through combinatorial therapy (Chaytow et al., 2021; Reilly et al., 2023). In this regard, identifying neurometabolic markers linked to disease severity and correlated with functional outcomes after treatment would be crucial for explaining differences in clinical responses and guiding discovery of new therapeutic approaches, including nutritional support. However, our current understanding of the biochemical and neurochemical abnormalities underlying SMA pathology and their specific response to SMN-inducing therapies remains very limited.

Studies in animal models revealed that cell-autonomous deficits in motor neurons alone cannot fully explain the disease phenotype. Instead, dysfunction in excitatory neuronal networks that control motor neuron output has emerged as a key contributor to SMA pathophysiology (Fletcher et al., 2017; Imlach et al., 2012; Lotti et al., 2012; Mentis et al., 2011; Simon et al., 2019). The best-characterized example is the dysfunction and loss of glutamatergic synapses from proprioceptive sensory neurons to motor neurons, which have emerged as some of the earliest manifestations of the disease in SMA mice (Fletcher et al., 2017; Ling et al., 2010; Mentis et al., 2011; Simon et al., 2019). The resulting reduction in afferent glutamatergic neurotransmission leads to down-regulation of Kv2.1 channels and decreased firing of SMA motor neurons, contributing to impaired muscle contraction and motor dysfunction (Fletcher et al., 2017). Consistent with SMA motor neurons suffering from reduced excitatory drive, increasing neuronal activity and glutamate signaling on motor neurons improve motor function in animal models of SMA (Biondi et al., 2010; Fletcher et al., 2017; Imlach et al., 2012; Simon et al., 2019). Importantly, recent studies have expanded the detrimental effects of SMN deficiency in neuronal networks beyond hypo-glutamatergic signaling to include monoaminergic neurotransmission (Delestrée et al., 2023; Pagiazitis et al., 2025; Valsecchi et al., 2023). However, it is unknown whether deficits in the metabolism of excitatory amino acids contribute to synaptic dysfunction in SMA sensory-motor circuits.

L-glutamate (L-Glu) is the most important excitatory amino acid in the central nervous system (CNS) (Curtis and Watkins, 1960; de Ceglia et al., 2023; Dingledine et al., 1999). It plays a pivotal role in orchestrating neurodevelopmental processes, synaptic transmission, and plasticity within the brain and spinal cord through stimulation of ionotropic and metabotropic receptors (mGluRs) (Bough et al., 2007; Mayer, 2005; Mayer, 2006; Squire and Bayley, 2007; Traynelis et al., 2010; Welby and Ebert, 2023). Besides neurotransmission, L-Glu controls fundamental cellular pathways, including non-essential amino acid synthesis and energy metabolism by directly regulating α-ketoglutarate levels and, in turn, the Krebs cycle (Tejero et al., 2024). The closely related dicarboxylic amino acid L-aspartate (L-Asp) and its D-enantiomer derivative D-Asp are also known to act as primary agonists of *N*-methyl D-aspartate receptors (NMDARs) (Dingledine et al., 1999; Errico et al., 2020; Mayer, 2006; Morland et al., 2013) and mGluR5 (Molinaro, 2015), while D-serine (D-Ser) functions in glutamatergic signaling by acting as an NMDAR co-agonist (Coyle et al., 2020; de Oliveira Souza et al., 2023). Lastly, L-glutamine (L-Gln) and L-Ser play a primary role in modulating the synthesis of L-Glu and D-Ser and, together with L-Asp, are involved in essential cellular processes including energy homeostasis, ammonium recycling, redox balance and in the biosynthesis of amino acids, nucleotides, and membrane lipids (Liu et al., 2023).

Despite their critical roles for neuronal and glial function, possible alterations in the levels of these neuroactive amino acids in the CNS of either SMA patients or animal models have not been investigated. Here, we addressed this question by performing a comprehensive neurotransmitter profiling in the spinal cord and brain of severe SMA mice as well as in the cerebrospinal fluid (CSF) of SMA patients across the spectrum of disease severity. We also investigated the impact of Nusinersen therapy on the CSF levels of excitatory amino acids and their precursors implicated in glutamatergic neurotransmission. Overall, our findings provide direct evidence for dysregulation of amino acid metabolism linked to glutamatergic neurotransmission that may contribute to motor dysfunction in severe SMA.

2. Results

2.1. SMN deficiency perturbs glutamate and serine metabolism in the CSF of severe SMA patients

We performed a real-world, retrospective study in two Italian Children's Hospitals to determine the effects of SMN deficiency on the concentration of neuroactive amino acids and their precursors in the CSF of untreated SMA patients across the disease-severity spectrum using HPLC (Fig. 1A). This analysis included CSF from SMA1 ($n = 34$), SMA2 ($n = 22$), and SMA3 ($n = 17$) patients as well as age-matched control subjects ($n = 7$) whose clinical and demographic features are presented in Table 1.

Using the non-parametric Kruskal-Wallis test, we found significant L-Glu and L-Gln changes in the CSF of SMA patients (L-Glu, $P = 0.007$; L-Gln, $P = 0.023$) (Fig. 1B,C; Suppl. Table 1). Importantly, further *post-hoc* comparisons highlighted a significant reduction of L-Glu in the CSF of SMA1 patients compared to controls (Fig. 1B; Suppl. Table 1). The L-Gln to L-Glu ratio was also significantly affected in SMA patients ($P = 0.005$; Kruskal-Wallis) (Fig. 1D; Suppl. Table 1). Accordingly, we found increased L-Gln/L-Glu ratio in both SMA1 and SMA2 patients compared to controls (respectively, $P = 0.006$ and $P = 0.036$; Mann-Whitney with Bonferroni correction) (Fig. 1D; Suppl. Table 1). In addition, the D-Ser to total Ser ratio – which is a reliable index of D-Ser metabolism (Hashimoto et al., 2005) – showed a significant difference among clinical conditions ($P < 0.001$; Kruskal-Wallis) (Fig. 1H and Suppl. Table 1). The following *post-hoc* analysis revealed an increased D-Ser/total Ser ratio in SMA1 patients compared to those with later-onset forms of SMA ($P < 0.001$; Fig. 1H; Suppl. Table 1). The Kruskal-Wallis test showed significant changes in L-Asp levels in SMA patients ($P = 0.037$) (Fig. 1E; Suppl. Table 1), and the CSF levels of D-Asp were below the detection

limit of our HPLC settings (0.01 pmol). Lastly, ANCOVA analysis performed on natural log-transformed data to evaluate the potential confounding effects of age and sex indicated that only variations in the levels of L-Glu ($P = 0.006$) and the L-Gln/L-Glu ratio ($P = 0.003$) were significantly associated with the clinical condition.

Lastly, we evaluated whether clinical interventions aimed at improving nutrition or respiration in SMA patients - including gastrostomy, non-invasive ventilation (NIV) and tracheostomy - might influence amino acid levels. Due to the lower number of SMA2 and SMA3 patients as well as the unbalanced distribution of those undergoing or not undergoing these interventions, we were only able to evaluate the most severe SMA1 patients. Statistical analysis revealed that none of these clinical factors significantly impacted the levels of any detected amino acid (Suppl. Table 2).

Overall, these findings show that SMN deficiency leads to significantly decreased concentrations of L-Glu in the CSF of severe SMA1 patients and to altered L-Gln to L-Glu conversion in both SMA1 and SMA2 patients. Additionally, they highlight an increased D-Ser to total Ser ratio in SMA1 patients compared to those with later-onset forms of the disease.

2.2. D-serine levels and D-serine/total serine ratio positively correlated with motor function in SMA1 patients

We next investigated whether the CSF concentrations of amino acids within each SMA patient type were associated with age or motor function assessed by CHOP-INTEND (SMA1) or HFMSE (SMA2 and SMA3) scales. Non-parametric Spearman's correlation analysis revealed that the levels of L-Glu and L-Gln, as well as the L-Gln/L-Glu ratio, showed no significant correlation with age or motor function in SMA1 patients (Table 2; Suppl Fig. 1). In contrast, D-Ser levels and the D-Ser/total Ser ratio were negatively correlated with age (Table 2; Suppl Fig. 2) and positively correlated with the CHOP-INTEND score (Table 2; Suppl. Fig. 3). Since we also found a negative correlation between age and the CHOP-INTEND score (Table 2; Suppl. Fig. 4), we performed multivariate linear regression analysis considering age as a confounding factor. This analysis did not confirm the significance of the association between D-Ser or D-Ser/total Ser ratio with the CHOP-INTEND score (respectively, $P = 0.074$ and $P = 0.203$), highlighting the putative influence of age on this correlation. In SMA2 patients, statistical analysis showed a significant negative correlation between D-Ser levels and the D-Ser/total Ser ratio with age (Table 2; Suppl. Fig. 2). There were also positive correlations of D-Ser levels and the D-Ser/total Ser ratio with the HFMSE score (Table 2; Suppl. Fig. 3), which failed to reach statistical significance probably due to the small sample size. Similar to SMA1 patients, age and motor function were negatively correlated in SMA2 individuals (Table 2; Suppl Fig. 4). In these patients, no significant correlation was found between HFMSE score and L-Glu, L-Gln levels or L-Gln/L-Glu ratio (Suppl. Fig. 1). In the late-onset SMA3 patients, we found a negative correlation of the D-Ser/total Ser ratio with age but not with the HFMSE score (Table 2; Suppl Figs. 2 and 3). Similarly, no significant correlations were found between this motor index score and L-Glu, L-Gln levels or L-Gln/L-Glu ratio (Suppl. Fig. 1). There was also no correlation between age and the HFMSE score (Table 2; Suppl. Fig. 4). No significant associations occurred between either D-Ser levels or the D-Ser/total Ser ratio and age in control subjects (Table 2; Suppl Fig. 2). However, previous research indicated a physiological age-dependent decrease in CSF D-Ser levels in healthy pediatric subjects after birth (Fuchs et al., 2006). Given this evidence, the lack of significant correlations observed in our study may be due to the limited sample size of the control group.

Overall, these results show a positive correlation between D-Ser levels or D-Ser/total Ser ratio and motor function. However, the confounding effects of age prevent us from drawing definitive conclusions

Table 1
Demographic and clinical characteristics of naïve SMA patients and control subjects enrolled in the study.

Demographic and clinical information	Controls ($n = 7$)	SMA1 (n = 34)	SMA2 (n = 22)	SMA3 (n = 17)
Sex (M:F, %)	43: 57	40: 60	41: 59	37: 63
Age, years	7.0 (4.0–12.0)	3.0 (0.7–4.9)	5.5 (2.0–11.8)	13.7 (7.6–17.2)
SMN copy number (2:3:4, %)		91:9:0	10:90:0	21.4: 64.3 14.3
BMI		13.4 (12.4–15.3)	17.9 (15.9–19.8)	19.4 (16.2–22.1)
CHOP-INTEND		14 (3–21)	–	–
HFMSE		–	9.5 (6.5–15)	52 (35–57)
Gastrostomy (Yes: No, %)		51: 49	0:100	0:100
NIV (Yes:No, %)		41: 59	33: 67	8: 92
Tracheostomy (Yes:No, %)		34:66	0: 100	0:100

Data are expressed as percentage frequencies or median (IQR). Abbreviations: BMI = Body Max Index; CHOP INTEND = Children's Hospital Of Philadelphia Infant Test Of Neuromuscular Disorders; HFMSE = Hammersmith Functional Motor Scale Expanded; NIV = Non-invasive ventilation.

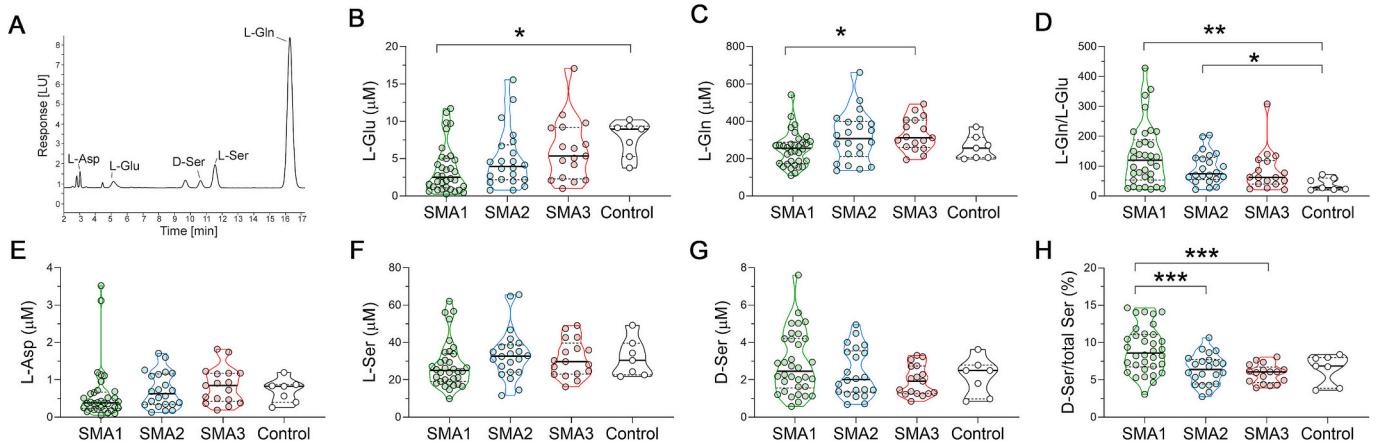

Fig. 1. Levels of neuroactive amino acids in the CSF of SMA patients and control individuals. (A) Representative chromatogram showing the peaks of L-aspartate (L-Asp), L-glutamate (L-Glu), D-serine (D-Ser), L-serine (L-Ser), and L-glutamine (L-Gln) in CSF of SMA1 patients. (B-H) Levels of L-Glu (B), L-Gln (C), L-Gln/L-Glu ratio (D), L-Asp (E), L-Ser (F), D-Ser (G) and D-Ser/total Ser percentage ratio (H) in the indicated cohorts of SMA1, SMA2 and SMA3 patients as well as control individuals. Data are shown as violin plots representing the median with interquartile range (IQR). *$P < 0.05$, **$P < 0.01$(Mann-Whitney test with Bonferroni's correction). Dots represent values from each individual analyzed.

Table 2
Correlation between amino acids and clinical or demographic variables in naïve SMA patients and control subjects.

		CHOP-INTEND/ HFMSE	L-Gln	L-Glu	L-Gln/ L-Glu	L-Asp	L-Ser	D-Ser	D-Ser/ total Ser
		ρ = −0.540	ρ = −0.026	ρ = −0.086	ρ = 0.171	ρ = 0.067	ρ = −0.044	ρ = −0.428	ρ = −0.720
	Age	***P* = 0.001**	*P* = 0.888	*P* = 0.641	*P* = 0.349	*P* = 0.714	*P* = 0.811	***P* = 0.015**	***P* < 0.001**
		n = 32	n = 32	n = 32	n = 32	n = 32	n = 32	n = 32	n = 32
SMA1			ρ = 0.07	ρ = 0.196	ρ = −0.243	ρ = 0.233	ρ = 0.116	ρ = 0.377	ρ = 0.452
	CHOP-INTEND	–	*P* = 0.971	*P* = 0.281	*P* = 0.180	*P* = 0.199	*P* = 0.528	***P* = 0.034**	***P* = 0.009**
			n = 32	n = 32	n = 32	n = 32	n = 32	n = 32	n = 32
		ρ = −0.638	ρ = 0.131	ρ = −0.034	ρ = 0.076	ρ = 0.073	ρ = −0.199	ρ = −0.470	ρ = −0.577
	Age	***P* = 0.002**	*P* = 0.571	*P* = 0.882	*P* = 0.743	*P* = 0.752	*P* = 0.388	***P* = 0.032**	***P* = 0.006**
		n = 20	n = 21	*n* = 21	n = 21	n = 21	n = 21	n = 21	n = 21
SMA2			ρ = 0.049	ρ = −0.032	ρ = 0.077	ρ = −0.328	ρ = 0.165	ρ = 0.378	ρ = 0.381
	HFMSE	–	*P* = 0.837	*P* = 0.892	*P* = 0.747	*P* = 0.158	*P* = 0.488	*P* = 0.100	*P* = 0.097
			n = 20	*n* = 20	n = 20	n = 20	n = 20	n = 20	n = 20
		ρ = 0.338	ρ = 0.178	ρ = −0.231	ρ = 0.270	ρ = −0.292	ρ = −0.257	ρ = −0.464	ρ = −0.692
	Age	***P* = 0.238**	*P* = 0.543	*P* = 0.427	*P* = 0.350	*P* = 0.311	*P* = 0.375	*P* = 0.095	***P* = 0.006**
		n = 14	*n* = 14	n = 14	n = 14	n = 14	n = 14	n = 14	n = 14
SMA3			ρ = 0.201	ρ = 0.020	ρ = 0.029	ρ = 0.174	ρ = 0.024	ρ = 0.082	ρ = 0.117
	HFMSE	–	*P* = 0.491	*P* = 0.946	*P* = 0.922	*P* = 0.551	*P* = 0.934	*P* = 0.781	*P* = 0.690
			n = 14	n = 14	n = 14	n = 14	n = 14	n = 14	n = 14
			ρ = 0.286	ρ = −0.321	ρ = 0.429	ρ = 0.071	ρ = −0.750	ρ = −0.714	ρ = −0.484
Controls	Age	–	*P* = 0.535	*P* = 0.482	*P* = 0.337	*P* = 0.879	*P* = 0.052	*P* = 0.071	*P* = 0.294
			n = 7	n = 7	n = 7	n = 7	n = 7	n = 7	n = 7

Non-parametric Spearman's rho coefficients (ρ) and related *P*-values (*P*) are indicated. Significant *P*-values are shown in bold. Abbreviations: CHOP-INTEND = Children's Hospital of Philadelphia Infant Test of Neuromuscular Disorders; HFMSE = Hammersmith Functional Motor Scale Expanded.

about the possible impact of these variations on motor improvement.

2.3. Nusinersen modulates glutamate, glutamine, and serine levels in the CSF of severe SMA patients

We next sought to determine the effects of Nusinersen treatment on the CSF levels of neuroactive amino acids and whether it could normalize the alterations observed in untreated, early-onset SMA patients. For this longitudinal analysis, we used a subgroup of SMA patients ($n = 18$ SMA1, $n = 17$ SMA2, and $n = 14$ SMA3) for whom CSF samples were available both prior to (T0) and 302 days after (T302) initiation of treatment, corresponding to the maintenance phase of Nusinersen therapy (Fig. 2A; Table 3).

The non-parametric Wilcoxon matched-pairs test revealed that

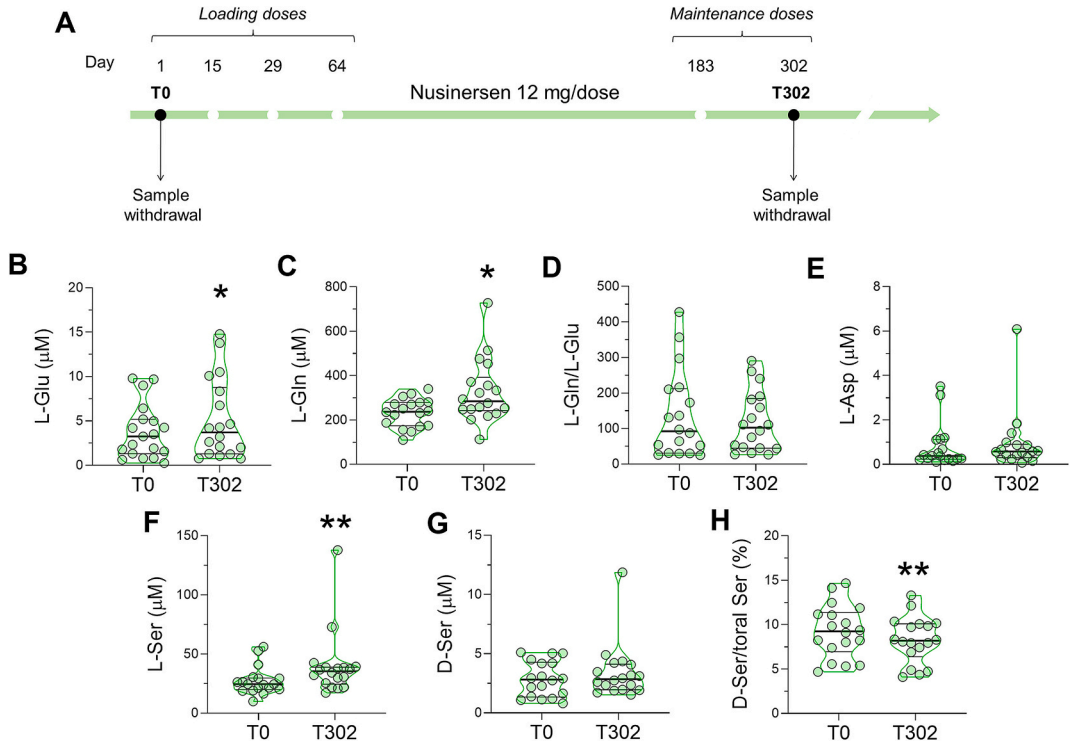

Fig. 2. Effect of Nusinersen on the levels of neuroactive amino acids in the CSF of SMA1 patients. (A) Schematic representation of the timeline of intrathecal Nusinersen administration and CSF collection in SMA patients. (B-H) Levels of L-glutamate (L-Glu) (B), L-glutamine (L-Gln) (C), L-glutamine/L-glutamate (L-Gln/L-Glu) ratio (D), L-aspartate (L-Asp) (E), L-serine (L-Ser) (F), D-serine (D-Ser) (G) and D-serine/total serine (D-Ser/total Ser) percentage ratio (H) in the CSF of SMA1 patients before treatment (T0, $n = 18$) and at the time of the sixth (T302, n = 18) injection of Nusinersen. *$P < 0.05$, **$P < 0.01$, compared to T0 (Wilcoxon matched-pairs signed ranks test). Data are shown as violin plots representing the median with interquartile range (IQR). Dots represent values from individual SMA1 patients.

Nusinersen significantly increased the levels of L-Glu ($P = 0.035$) and L-Gln ($P = 0.025$) in the CSF of SMA1 patients relative to the corresponding drug-free baseline (Fig. 2B, C; Suppl. Table 3). Moreover, Nusinersen administration significantly increased L-Ser levels ($P = 0.004$) and decreased the D-Ser/total Ser ratio in the CSF of SMA1 patients ($P = 0.007$) (Fig. 2F, H; Suppl. Table 3). In SMA2 patients, we did not observe significant changes in the concentration of neuroactive amino acids after Nusinersen treatment (Suppl. Fig. 5; Suppl. Table 3). In SMA3 patients, Nusinersen treatment decreased the CSF levels of several amino acids, which differs from its effects in both SMA1 and SMA2 patients. Accordingly, we found lower levels of L-Glu ($P = 0.006$) resulting in a slight increase in the L-Gln/L-Glu ratio ($P = 0.019$) as L-Gln levels were comparable between groups ($P = 0.064$) (Suppl. Fig. 6 A-C; Suppl. Table 3). Additionally, there were reduced levels of L-Ser ($P = 0.019$), D-Ser ($P = 0.016$), and L-Asp ($P = 0.038$) in Nusinersen-treated SMA3 patients relative to baseline (Suppl. Fig. 6D-F; Suppl. Table 3).

We also assessed whether gastrostomy, NIV and tracheostomy might influence amino acid levels in Nusinersen-treated SMA1 patients. Similarly to untreated patients, we found that these clinical interventions did not affect any detected amino acid levels in SMA1 patients treated with Nusinersen (Suppl. Table 2).

Overall, these results reveal that Nusinersen-induced upregulation of SMN modulates the concentrations of L-Glu, L-Gln, and L-Ser while decreasing the D-Ser/total Ser ratio in the CSF of SMA1 patients. This effect partially counteracts the amino acid dysregulation associated with the severe form of the disease prior to treatment.

2.4. D-serine/total serine ratio in SMA1 and the levels of L-serine and D-serine in SMA2 are positively correlated with motor function after Nusinersen therapy

We next investigated the association between changes in amino acid levels and the demographic and clinical parameters of SMA patients after 302 days of Nusinersen treatment. Non-parametric Spearman's correlation analysis highlighted a positive correlation between the D-Ser/total Ser ratio and the CHOP-INTEND score but no significant correlation with age in Nusinersen-treated SMA1 patients (Suppl. Fig. 7; Table 4). However, when controlling for age using multivariate linear regression, the association between D-Ser/total Ser and CHOP-INTEND score was no longer significant ($P = 0.136$). As expected for the early-onset severe form of the disease, we found a negative correlation between age and CHOP-INTEND score in SMA1 **patients (**Table 4**)**. In Nusinersen-treated SMA2 patients, we found a positive correlation of L-Ser and D-Ser levels with HFMSE score (Suppl. Fig. 8–9; Table 4). Specifically, L-Ser and D-Ser levels were negatively correlated with age, which was also negatively correlated with HFMSE score **(**Table 4**)**. However, after multivariate linear regression analysis, only age but not L-Ser or D-Ser remained significantly associated with HFMSE (L-Ser: $P = 0.308$; D-Ser: $P = 0.809$). Moreover, statistical analysis showed only a negative correlation between the D-Ser/total Ser ratio and the age in Nusinersen-treated SMA3 patients (Table 4).

Taken together, these results highlight positive correlations between D-Ser/total Ser and CHOP-INTEND in SMA1, and between L-Ser or D-Ser and HFMSE in SMA2. However, similar to untreated SMA patients, the impact of age on motor function in early-onset SMA patients complicates the interpretation of the observed amino acid variations in relation to motor outcome.

Table 3
Clinical and demographic characteristics of SMA patients treated with Nusinersen.

Demographic and clinical information	SMA1 (n = 18)	SMA2 (n = 17)	SMA3 (n = 14)
Sex (M:F, %)	39: 61	30: 70	30: 70
Age	2.7 (0.7–4.9)	5.5 (3.1–11.8)	13 (9–16)
SMN copy number (2:3:4, %)	94:6:0	94:6:0	23:63:14
BMI	13.2 (11.7–14.6)	18.2 (16.3–19.8)	19.4 (16.2–22.1)
CHOP-INTEND	6.5 (3–17)		
HFMSE		9 (8–13)	55 (36–56)
Gastrostomy (Yes:No, %)	66:34	0:100	0/100
NIV (Yes:No, %)	39: 61	35:65	8:92
Tracheostomy (Yes:No, %)	33: 67	0:100	0:100

Data are expressed as percentage frequencies or median (IQR). Abbreviations: BMI = Body Max Index; CHOP INTEND = Children's Hospital Of Philadelphia Infant Test Of Neuromuscular Disorders; HFMSE = Hammersmith Functional Motor Scale Expanded; NIV = Non-invasive ventilation.

2.5. Dysregulation of glutamine/glutamate ratio in the brain and spinal cord of SMA mice

To expand on our investigation of the effects of SMN deficiency on the levels of neuroactive amino acids, we conducted HPLC analysis (Fig. 3B) in brain and spinal cord tissues isolated from SMA mice at early (postnatal day 3, P3) and late (P11) symptomatic stages of the disease. SMN depletion did not change the levels of any amino acid tested in the brain or spinal cord from SMNΔ7 mice compared with WT at P3 (Fig. 3C, D; Suppl. Fig. 9; Suppl. Table 4). In contrast, we found a significant increase in the concentration of L-Gln and L-Gln/L-Glu ratio in both the brain and spinal cord of SMNΔ7 mice compared to WT at P11 (Fig. 3E,F; Suppl. Fig. 10; Suppl. Table 4). Furthermore, SMNΔ7 mice displayed an increased D-Asp/total Asp ratio in the spinal cord at P11 (Suppl. Fig. 10; Suppl. Table 4).

We then used two-way ANOVA followed by Tukey's *post-hoc* comparisons to further analyze the neurochemical variations during postnatal CNS development in WT and SMNΔ7 mice. This highlighted a physiological, age-dependent drop of the L-Gln/L-Glu ratio in the brain of WT mice that does not occur in SMNΔ7 mice, resulting in a higher L-Gln/L-Glu ratio in SMNΔ7 relative to WT mice at P11 (Fig. 3G; Suppl. Table 5). Similarly, we found that the L-Gln/L-Glu ratio in the spinal cord of SMNΔ7 mice significantly increased relative to WT littermates at P11 (Fig. 3H; Suppl. Table 5). Furthermore, despite significant age-dependent changes between WT and SMNΔ7 mice were found for the D-Ser/total Ser ratio in the brain and the D-Asp/total Asp ratio in the spinal cord, no differences were highlighted between genotypes at each single time point using the Tukey's multiple comparisons *post-hoc* analysis (Suppl. Fig. 11, Suppl. Table 5).

These findings indicate that SMN deficiency significantly impacts the metabolism of neuroactive amino acids involved in glutamatergic neurotransmission in the brain and spinal cord of SMA mice at the disease end stage. Importantly, the increase in the L-Gln/L-Glu ratio emerges as a conserved signature of neurochemical dysregulation in the CSF of severe SMA patients and the CNS of mouse models.

2.6. D-serine supplementation moderately improves motor function in SMA mice

The results of our neurochemical profiling highlighted the dysregulation of amino acid metabolism acting on glutamatergic neurotransmission as well as a potential correlation between higher D-Ser/total Ser ratio in the CSF and better motor function in severe SMA patients. Since D-Ser is a major co-agonist of NMDARs (Coyle et al., 2020; de Oliveira Souza et al., 2023), we sought to investigate the phenotypic effects of increasing D-Ser levels in the CNS of SMA mice.

First, to validate that intraperitoneal (IP) administration of D-Ser increases its levels in the mouse spinal cord, we performed a single injection of vehicle or D-Ser at a dosage of 500 mg/kg in WT mice at P3 followed by HPLC analysis 1 h post-injection (Fig. 4A). This dose was selected based on previous studies indicating that D-Ser administration in the range of 300–1000 mg/kg is both effective in producing functional effects and non-toxic in mice (Hashimoto et al., 2009; Meftah et al., 2021; Nilsson et al., 1997; Nomura et al., 2016). Accordingly, we found that the concentration of D-Ser (median [IQR] of nmol/mg of

Table 4
Correlation between amino acids and clinical or demographic variables in SMA patients before and after Nusinersen treatment.

Patients	Therapy phase	Parameter	CHOP-INTEND / HFMSE	L-Gln	L-Glu	Gln/Glu	L-Asp	L-Ser	D-Ser	D-Ser/tot Ser
SMA1 (N = 18)	T0	Age	ρ = −0.636 **P = 0.005**	ρ = 0.084 P = 0.741	ρ = 0.071 P = 0.779	ρ = 0.018 P = 0.945	ρ = 0.237 P = 0.343	ρ = −0.005 P = 0.984	ρ = −0.344 P = 0.162	ρ = −0.649 **P = 0.004**
		CHOP-INTEND	–	ρ = 0.113 P = 0.656	ρ = 0.292 P = 0.240	ρ = −0.326 P = 0.187	ρ = 0.325 P = 0.188	ρ = 0.257 P = 0.304	ρ = 0.408 P = 0.093	ρ = 0.389 P = 0.110
	T302	Age	ρ = −0.735 **P = 0.001**	ρ = 0.141 P = 0.576	ρ = 0.189 P = 0.453	ρ = 0.001 P = 0.997	ρ = 0.352 P = 0.152	ρ = −0.005 P = 0.984	ρ = −0.257 P = 0.303	ρ = −0.364 P = 0.137
		CHOP-INTEND	–	ρ = −0.303 P = 0.237	ρ = −0.225 P = 0.386	ρ = −0.039 P = 0.881	ρ = −0.184 P = 0.479	ρ = −0.139 P = 0.596	ρ = 0.264 P = 0.306	ρ = 0.528 **P = 0.030**
SMA2 (N = 17)	T0	Age	ρ = −0.511 **P = 0.036**	ρ = 0.020 P = 0.940	ρ = 0.025 P = 0.926	ρ = −0.065 P = 0.804	ρ = 0.040 P = 0.877	ρ = −0.207 P = 0.425	ρ = −0.415 P = 0.098	ρ = −0.471 P = 0.056
		HFMSE	–	ρ = 0.102 P = 0.696	ρ = −0.119 P = 0.648	ρ = 0.217 P = 0.404	ρ = −0.437 P = 0.079	ρ = 0.053 P = 0.840	ρ = 0.233 P = 0.369	ρ = 0.177 P = 0.496
	T302	Age	ρ = −0.845 **P < 0.001**	ρ = −0.422 P = 0.091	ρ = −0.329 P = 0.197	ρ = −0.145 P = 0.579	ρ = −0.188 P = 0.471	ρ = −0.677 **P = 0.003**	ρ = −0.729 **P = 0.001**	ρ = −0.218 P = 0.400
		HFMSE	–	ρ = 0.402 P = 0.109	ρ = 0.330 P = 0.196	ρ = 0.028 P = 0.914	ρ = 0.098 P = 0.707	ρ = 0.522 **P = 0.032**	ρ = 0.568 **P = 0.017**	ρ = 0.038 P = 0.884
SMA3 (N = 13)	T0	Age	ρ = 0.337 P = 0.259	ρ = 0.206 P = 0.499	ρ = −0.124 P = 0.687	ρ = 0.157 P = 0.609	ρ = −0.217 P = 0.476	ρ = −0.248 P = 0.415	ρ = −0.437 P = 0.135	ρ = −0.710 **P = 0.007**
		HFMSE	–	ρ = 0.210 P = 0.491	ρ = 0.017 P = 0.957	ρ = 0.039 P = 0.900	ρ = 0.210 P = 0.491	ρ = 0.033 P = 0.914	ρ = 0.110 P = 0.719	ρ = 0.110 P = 0.719
	T302	Age	ρ = 0.262 P = 0.388	ρ = 0.393 P = 0.184	ρ = 0.025 P = 0.936	ρ = 0.165 P = 0.590	ρ = 0.201 P = 0.511	ρ = 0.044 P = 0.886	ρ = −0.105 P = 0.734	ρ = −0.746 **P = 0.003**
		HFMSE	–	ρ = 0.536 P = 0.059	ρ = 0.377 P = 0.204	ρ = −0.094 P = 0.761	ρ = 0.198 P = 0.517	ρ = 0.272 P = 0.368	ρ = 0.358 P = 0.230	ρ = 0.039 P = 0.901

Non-parametric Spearman's rho coefficients (ρ) and related *P*-values (*P*) are indicated. Significant *P*-values are shown in bold. Abbreviations: CHOP-INTEND = Children's Hospital of Philadelphia Infant Test of Neuromuscular Disorders; HFMSE = Hammersmith Functional Motor Scale Expanded.

protein, D-Ser = 28.97 [25.29–58.61] *vs* vehicle = 2.81 [2.71–3.09], *P* = 0.0286, Mann-Whitney test) and the D-Ser/total Ser ratio (D-Ser = 51.90 [47.54–67.22] *vs* vehicle = 11.02 [10.34–11.68], *P* = 0.0286) were significantly increased in the spinal cord of D-Ser-injected mice relative to control mice injected with vehicle (Fig. 4A-C).

Next, we analyzed the *in vivo* effects of daily supplementation of D-Ser (500 mg/kg) starting at birth on SMN expression and the phenotype of SMA mice, which included daily measures of weight gain, motor function, and survival. Western blot analysis of spinal cord tissue isolated at P11 from WT and SMA mice either with or without amino acid supplementation demonstrated that D-Ser does not increase SMN protein levels (Fig. 4D,E). Interestingly, phenotypic analysis showed a moderate improvement of motor function assessed by the righting reflex in D-Ser-treated relative to untreated SMA mice (Fig. 4F; Suppl. Table 6). This motor benefit appeared in the second postnatal week and was not associated with an increase in weight gain, which was similar for D-Ser-treated and untreated SMA mice (Fig. 4G). Lastly, despite fewer early deaths and some slightly longer-lived mice being noted, treatment with D-Ser did not increase the median survival of SMA mice (Fig. 4H).

Overall, these results are consistent with the possibility that increased CNS levels of D-Ser may partially improve motor function in a mouse model of SMA by enhancing NMDAR-dependent neurotransmission.

3. Discussion

Selective degeneration of motor neurons and skeletal muscle atrophy are hallmarks of SMA in both patients and mouse models (Tisdale and Pellizzoni, 2015; Wirth et al., 2020). However, cell-autonomous deficits in motor neurons alone cannot fully explain the SMA phenotype and dysfunction of neuronal networks that control motor output has been implicated in disease etiology (Tisdale and Pellizzoni, 2015). Accordingly, several studies have shown that reduced excitatory drive to motor neurons (Fletcher et al., 2017; Imlach et al., 2012; Lotti et al., 2012; Mentis et al., 2011; Simon et al., 2019) and metabolic dysfunction in fundamental intracellular pathways (Errico et al., 2022) may play a role in SMA pathophysiology. Nevertheless, while a variety of synaptic deficits in motor neuron afferents have been documented (Buettner et al., 2021; Delestrée et al., 2023; Fletcher et al., 2017; Mentis et al., 2011; Pagiazitis et al., 2025; Simon et al., 2019), whether SMN deficiency directly alters the content of neurotransmitters in the CNS of animal models and SMA patients is unknown. Here, we addressed this issue by investigating changes in the levels of the most abundant excitatory D- and L-amino acids, which either drive glutamatergic synapse activity or act as their immediate precursors in the CNS of SMNΔ7 mice and in the CSF of SMA patients of differing severity both before and after Nusinersen therapy.

Our findings reveal that SMN deficiency is associated with prominent dysregulation of D- and L-amino acids involved in glutamatergic neurotransmission in the CSF of severe SMA patients as well as in the brain and spinal cord of SMNΔ7 mice. Accordingly, we found lower levels of L-Glu in SMA1 patients and a trend toward reduction in SMA2 and SMA3 patients compared to controls. L-Glu reduction also results in a significant increase of the L-Gln/L-Glu ratio in both SMA1 and SMA2 patients compared to control subjects. Interestingly, a significant increase in the L-Gln/L-Glu ratio also occurs in the brain and spinal cord of SMNΔ7 mice at late symptomatic stages. Thus, deregulated L-Gln/L-Glu ratio emerges as a neurochemical signature of altered glutamatergic metabolism common to both SMA1 and SMA2 patients and animal models in the late stage of the disease. Together with the dysfunction

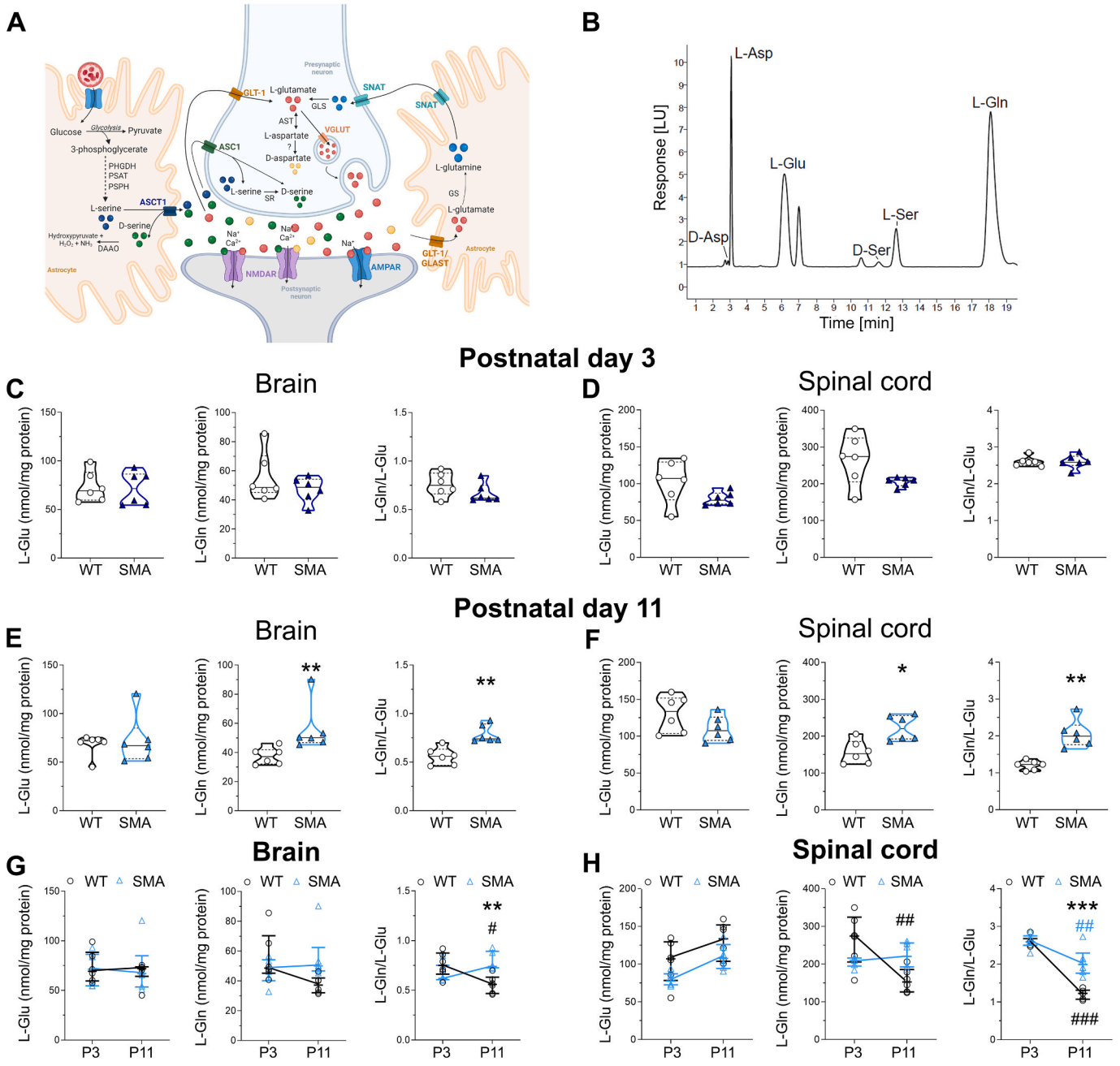

Fig. 3. Analysis of neuroactive amino acid levels in the brain and spinal cord of SMNΔ7 mice at early and late symptomatic stage of the disease. A) Schematic model of the tripartite glutamatergic synapse showing the main localization of the amino acids analyzed in this study. Image created with BioRender.com (www.biorender.com). Abbreviations: PHGDH: phosphoglycerate dehydrogenase; PSAT: phosphoserine aminotransferase; PSPH: phosphoserine phosphatase; DAAO: D-amino acid oxidase; SR: serine racemase; GLS: glutaminase; GS: glutamine synthetase; ASCT1: alanine, serine, cysteine transporter 1; ASC1: alanine, serine, cysteine transporter 1; GLT-1: glutamate transporter 1; SNAT: sodium-coupled neutral amino acid transporter; GLAST: glutamate aspartate transporter; NMDAR: *N*-methyl-D-aspartate receptor; AMPAR: alpha-amino-3-hydroxy-5-methyl-4-isoxazolepropionic acid receptor; VGLUT: vesicular glutamate transporter. B) Representative chromatogram showing the peaks of L-aspartate (L-Asp), L-glutamate (L-Glu), D-serine (D-Ser), L-serine (L-Ser), and L-glutamine (L-Gln) in the brain homogenate of SMNΔ7 mice. (C-F) Levels of L-Glu, L-Gln and L-Gln/L-Glu ratio in the brain and spinal cord of wild type (WT) and SMNΔ7 mice at postnatal day 3 (P3), and P11. The average amounts of amino acids detected were normalized for mg of total proteins. Dots represent values from individual mice. Amino acid levels are expressed as violin plots representing median with interquartile range (IQR) and analyzed by Mann-Whitney test (*$P < 0.05$, **$P < 0.01$, compared to age-matched WT mice). (G,H) Amino acid levels were also analyzed as two-way ANOVA, followed by Tukey's multiple comparisons test (**$P < 0.01$, **$P < 0.0001$, compared to age-matched WT mice; $^{\#\#}P < 0.01$, $^{\#\#\#}P < 0.0001$, compared to genotype-matched P3 mice). Amino acid levels were shown as scatter dot plots representing median with interquartile range (IQR) while dots represent values from individual mice.

and loss of glutamatergic synapses impinging on motor neurons (Fletcher et al., 2017; Ling et al., 2010; Mentis et al., 2011; Simon et al., 2019), and consistent with the beneficial effects of increased glutamatergic stimulation on motor function in SMA animal models (Biondi et al., 2010; Fletcher et al., 2017; Imlach et al., 2012; Simon et al., 2021), it is plausible that the dysfunction of L-Glu metabolism may reflect the excitatory neurotransmission defects characteristic of the disease state.

The SMA-related changes in the L-Gln/L-Glu ratio are suggestive of abnormalities in the glutamate-glutamine cycle, an imbalance of which

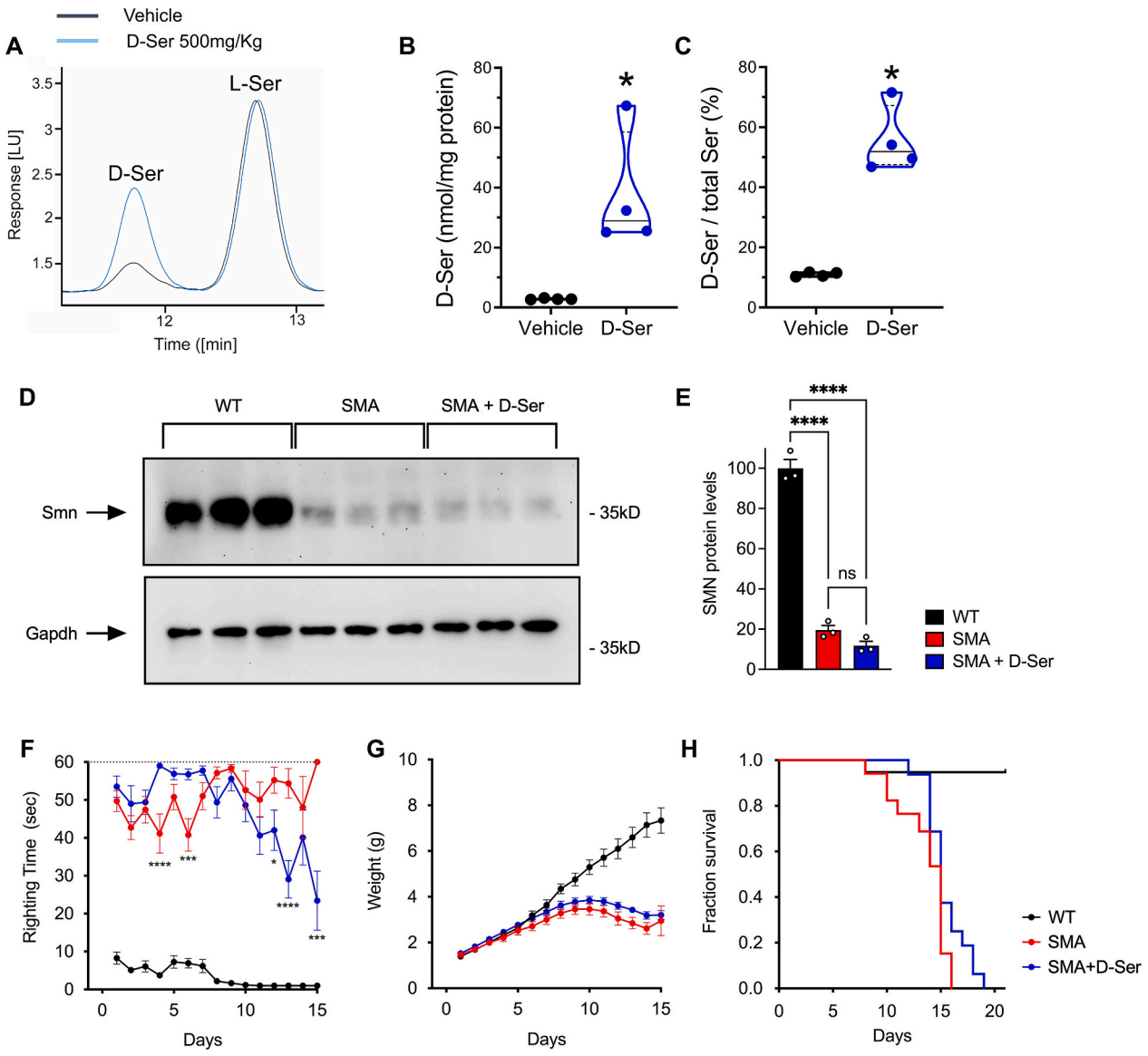

Fig. 4. SMN-independent amelioration of motor function by D-serine supplementation in SMA mice. (A) Representative chromatogram showing the peaks of D-serine (D-Ser) and L-serine (L-Ser) in the spinal cord homogenate of SMNΔ7 mice after a single injection of vehicle (black line) or 500 mg/kg D-Ser treatment (blu line) at P3. (B-C) D-Ser levels and D-Ser/toral Ser ratio in the spinal cord of WT mice treated with a single injection of 500 mg/kg D-serine compared to vehicle-treated mice at P3. *$P < 0.05$, compared to vehicle (Mann-Whitney test) (D) Western blot analysis of SMN protein levels in spinal cords from WT and either untreated or D-Ser-treated SMNΔ7 mice at P11. GAPDH was probed as a loading control. Three independent mice per group were analyzed. (E) Quantification of SMN levels normalized to GAPDH from the data in (D). Ordinary one-way ANOVA with Šídák's multiple comparisons test. ****$P < 0.0001$, ns: not significant. Values are means and SEM. (F-H) Analysis of righting time (F), body weight (G), and survival (H) in WT mice ($n = 19$) and either untreated ($n = 17$) or D-Ser-treated ($n = 16$) SMNΔ7 mice. Two-way ANOVA with Tukey's multiple comparisons test. ****$P < 0.0001$, ***$P < 0.001$, *$P < 0.05$. Values are means and SEM (see also Suppl. Table 6 for raw data).

has been associated with various neurological and psychiatric disorders (Leo et al., 2022). This cycle involves the functional interaction between neurons and astrocytes in the tripartite glutamatergic synapse where pre- and post-synaptic nerve terminals and perisynaptic astrocytic processes recycle L-Glu for neurotransmission (Fig. 3A). Following synaptic release, L-Glu binds to ionotropic and metabotropic glutamate receptors located post-synaptically and is then taken up by astrocytes *via* excitatory amino acid transporters to prevent excitotoxicity caused by excessive activation of glutamate receptors (Malik and Willnow, 2019). In astrocytes, the enzyme glutamine synthetase converts the main part of L-Glu into L-Gln, which is shuttled to the neuron *via* sodium-coupled neutral amino acid transporters. L-Gln is then deaminated to L-Glu by glutaminase in the mitochondria of neurons and either transferred by vesicular glutamate transporters into synaptic vesicles for the further rounds of neurotransmission or converted in α-ketoglutarate for Krebs cycle activity (Andersen et al., 2021; Dienel, 2013). Thus, in addition to perturbing glutamatergic neurotransmission, SMN deficiency may also trigger an abnormally increased conversion of L-Glu in α-ketoglutarate into the Krebs cycle as a compensatory mechanism to counteract the pervasive energy failure due to mitochondrial abnormalities associated with SMA (Zilio et al., 2022). Importantly, previous *in vitro* and *in vivo* studies have highlighted several deficits induced by SMN deficiency in SMA astrocytes that may contribute to the dysfunction of the tripartite synapse and the neurochemical alterations observed here (Abati et al., 2020; Martin et al., 2017; Ohuchi et al., 2019; Rindt et al., 2015).

In line with the deregulated L-Gln/L-Glu ratio observed in the brain and spinal cord of SMA mice at late symptomatic stages, previous studies demonstrated that astrogliosis progressively becomes more widespread from the early to late symptomatic stages of the disease in the spinal cord of SMA mice (Rindt et al., 2015). Regardless of specific nervous cell

contributions, future studies are needed to ascertain the extent to which L-Glu metabolic dysfunction is a direct consequence of SMN reduction or arises from indirect mechanisms secondary to the disease. We hypothesize that alterations in L-Gln/L-Glu conversion, which specifically occur in severe SMA patients and late-symptomatic SMA mice, reflect the emergence of astrogliosis, synaptopathy and defective energy metabolism that prevails during the advanced stages of the disease (Deguise et al., 2021; Hamilton and Gillingwater, 2013; Ohuchi et al., 2019; Rindt et al., 2015; Shababi et al., 2014).

Our neurochemical profiling revealed an upregulation of the D-Ser/total Ser ratio in the CSF of SMA1 patients compared to those with SMA2 and SMA3, reflecting opposite trends toward decrease or increase of L-Ser and D-Ser levels, respectively. Based on the pharmacological properties of D-Ser as a potent endogenous co-agonist of NMDARs (Coyle et al., 2020; de Oliveira Souza et al., 2023), these findings further extend the link between SMN deficiency and dysregulation of amino acid metabolism acting on glutamatergic neurotransmission in severe SMA. As is the case for the glutamate-glutamine cycle described above, an increase in the D-Ser/total Ser ratio points to dysfunction of astrocyte metabolism in SMA1 patients. Accordingly, *de novo* synthesis of L-Ser in the CNS occurs exclusively in astrocytes through the phosphorylated pathway, which employs 3-phosphoglycerate generated by glycolysis; L-Ser is then shuttled to neurons for the biosynthesis of D-Ser catalyzed by serine racemase (SR) (Murtas et al., 2020; Wolosker and Radzishevsky, 2013) (Fig. 3A). Interestingly, our clinical data highlight a positive correlation between D-Ser levels or the D-Ser/total Ser ratio and motor function assessed by CHOP-INTEND in SMA1 patients and a similar trend in SMA2 patients assessed by HFSME. However, the correlation between D-Ser metabolism and motor function should be interpreted cautiously due to the potentially confounding effect of age. Accordingly, age was negatively correlated with D-Ser levels, the D-Ser/total Ser ratio, and motor function in SMA1 and SMA2 patients; and age-adjusted partial correlation and multiple regression analyses did not confirm the association between D-Ser metabolism and clinical scores. The inverse correlation of D-Ser levels or the D-Ser/total Ser ratio with age observed in the CSF of SMA patients and controls is in agreement with previous observations in a large cohort of pediatric individuals (Fuchs et al., 2006). Moreover, while the mechanisms remain to be established, it is worth noting that dysregulation of serine metabolism has been found in other neurological disorders, including Alzheimer's disease, Parkinson's disease, amyotrophic lateral sclerosis (ALS), dementia, and frailty (Di Maio et al., 2023; Imarisio et al., 2024a; Imarisio et al., 2024b; Orzylowski et al., 2021; Piubelli et al., 2021; Sasabe et al., 2007).

Our longitudinal analysis of the neurochemical composition of the CSF in SMA patients before and after Nusinersen treatment further supports the role of SMN in regulating the concentration of D- and L-amino acids that modulate glutamatergic neurotransmission, especially in patients with the most severe form of the disease. Accordingly, we found that Nusinersen induces a significant increase in the levels of L-Glu and L-Gln as well as upregulation of L-Ser with consequent reduction of the D-Ser/total Ser ratio in the CSF of treated SMA1 patients relative to their drug-free baseline. These findings are consistent with previous untargeted metabolomic studies that highlight the effect of Nusinersen on glutamate metabolism in SMA1 patients (Errico et al., 2022). This effect was accompanied by modulation of energy-related Krebs cycle and glutathione metabolism, which depend on direct L-Glu supply. Hence, these results link Nusinersen-dependent SMN upregulation to an improved astrocyte-dependent metabolism of amino acids related to glutamatergic neurotransmission and energy metabolism, which are significantly affected in severe SMA (Hernandez-Gerez et al., 2020; Walter et al., 2018). Interestingly, in contrast to SMA1 patients, Nusinersen did not affect the levels of neuroactive amino acids in the CSF of SMA2 patients and slightly decreased the concentration of L-Glu, L-Asp, L-Ser, D-Ser as well as the L-Gln/L-Glu ratio in SMA3 patients. The opposite effects of Nusinersen in modulating the CSF concentrations of L-Glu and L-Ser in SMA1 and SMA3 patients confirm and extend our previous observations that the impact of SMN upregulation on amino acid metabolism and the expression of neuroinflammatory markers follows distinct trajectories depending on SMA severity (Errico et al., 2022; Nuzzo et al., 2023; Valsecchi et al., 2023). In keeping with this, disease severity and the stage of SMA progression appear to be critical factors guiding specific metabolic responses to Nusinersen treatment.

Lastly, we found a positive correlation of motor function with the D-Ser/total Ser ratio in SMA1 patients and with the levels of L-Ser or D-Ser in SMA2 patients after 302 days of Nusinersen treatment. However, similar to the analysis in naïve SMA patients, it remains unclear whether these neurochemical differences are directly associated with motor improvement as age is a significant confounding factor in these correlations. Nevertheless, it is important to highlight that L-Ser supplementation is currently used in the therapy of the Neu-Laxova syndrome, characterized by severe peripheral malformations and microcephaly (van der Crabben et al., 2013), and in Phase I clinical trials for the treatment of an inherited form of peripheral neuropathy (Garofalo et al., 2011) and ALS (Levine et al., 2017). Future longitudinal studies in larger cohorts of SMA patients and age-matched healthy individuals will help to address the issue.

Given the difficulty in conclusively establishing cause-effect relationships between changes in the CSF levels of neuroactive amino acids and clinical outcomes in SMA patients, we sought to initially address this issue in a preclinical *in vivo* setting by studying the phenotypic effects of D-Ser metabolism modulation in a mouse model of SMA. The focus on D-Ser was prompted by our observations that the D-Ser/total Ser ratio in the CSF of SMA1 patients i) is higher compared to that of SMA2 and SMA3 patients, ii) positively correlates with motor function, and iii) decreases after Nusinersen therapy. If changes in the D-Ser/total Ser ratio are biologically relevant to SMA pathology, two main scenarios can be envisioned that take into consideration the role of D-Ser as a potent co-agonist of NMDAR (Coyle et al., 2020; de Oliveira Souza et al., 2023). On one hand, increased levels of D-Ser may be beneficial and reflect a homeostatic attempt to counteract deficits in glutamatergic neurotransmission at NMDARs through enhanced L-Ser to D-Ser conversion, which is tuned down after Nusinersen treatment enhances L-Glu levels. On the other hand, increased levels of endogenous D-Ser could be harmful to neurons *via* excitotoxicity – a possibility consistent with previous studies of the motor neuron disease ALS (Mitchell et al., 2010; Sasabe et al., 2007; Sasabe et al., 2011). Strikingly, our results show that systemic daily supplementation of D-Ser in severe SMA mice ameliorates motor function while having no effects on weight gain and survival. Furthermore, the motor improvement is independent from SMN whose low expression levels in the spinal cord are unaffected by D-Ser. These findings suggest the possibility that elevated D-Ser levels do not have deleterious but rather beneficial effects on the severe motor phenotype of SMA mice by enhancing glutamatergic neurotransmission at the GluN1 subunit of NMDARs. This interpretation is in agreement with previous studies showing that physical and pharmacological approaches aimed at increasing neuronal activity and NMDAR signaling improve motor function in animal models of SMA (Biondi et al., 2010; Biondi et al., 2008; Branchu et al., 2013; Fletcher et al., 2017; Imlach et al., 2012; Simon et al., 2021).

The reduction of neurological defects observed with D-Ser supplementation in SMA mice, along with the neurochemical findings in severe SMA patients before and after Nusinersen, highlight the potential of this atypical amino acid as a therapeutic target and encourage exploration of combinatory therapeutic strategies in future clinical trials. In this context, clinical studies have shown that even higher D-Ser doses are both safe and effective (Meftah et al., 2021). According to the current mechanistic understanding of the pathogenic effects of reduced glutamatergic drive in SMA motor circuits (Fletcher et al., 2024; Fletcher et al., 2017; Simon et al., 2024), it is conceivable that increased NMDAR activation by D-Ser could counteract synaptic imbalance, enhance membrane expression of Kv2.1, and increase firing in motor neurons. However, additional pre-clinical studies are needed to establish the

mechanism of action and translational value of D-Ser supplementation in SMA. These include testing the effects of increased D-Ser levels on synaptic connectivity and function of sensory-motor circuits either alone or in combination with SMN-inducing drugs as well as evaluating the efficacy of different dosing regimens.

Overall, this is the first comprehensive study to thoroughly characterize the presence and variations of neuroactive amino acids, including D-configured amino acids like D-Ser and D-Asp, in the context of SMA. Additionally, this study holds significant translational value and it is the first to perform neurochemical analyses in both the CSF of SMA patients from two different hospitals, before and after Nusinersen therapy, and in the CNS (brain and spinal cord) of SMA mice at various stages of disease progression. This dual and longitudinal approach offers unprecedented insights into the disease, bridging clinical and preclinical findings.

In conclusion, the present findings reveal that SMN deficiency disrupts the physiological balance of neuroactive D- and L-amino acids linked to glutamatergic receptors signaling in the CNS of SMA mice and the CSF of severe SMA patients. The resulting defects may compound the deleterious effects associated with the loss of excitatory synapses on motor neurons in spinal sensory-motor circuits as well as interfere more broadly with glutamatergic neuronal networks in the brain of severe SMA patients, including cognitive deficits. Moreover, our findings identify the modulation of glutamate and serine metabolism as downstream targets of Nusinersen treatment in SMA patients. This supports further investigation into pharmacological approaches, such as D-Ser supplementation, aimed at improving glutamatergic neurotransmission deficits for use in combination therapies with SMN-inducing drugs.

4. Materials and methods

4.1. Patients' characteristics

This is a two-center study (IRCCS Bambino Gesù Hospital, Rome, Italy; IRCCS Istituto Giannina Gaslini, Genoa, Italy) conducted on seventy-three patients affected by SMA1 ($n = 34$), SMA2 ($n = 22$) and SMA3 ($n = 17$) who received intrathecal treatment with Nusinersen (12 mg) (Table 1). Additionally, seven non-neurological pediatric control subjects aged 2.5–14 years were included in the study (Table 1). Control subjects underwent CSF withdrawal for suspected meningitis. The study was approved by the local Ethics Committees of the two Hospitals (2395_OPBG_2021). All participants and/or their legal guardians signed a written informed consent. CSF samples were collected at day 0 (T0; baseline) and day 302 (T302; after 5 Nusinersen injections) and used for the detection of amino acids. For SMA1 patients, we collected n = 34 CSF samples at T0, and $n = 18$ at T302. For SMA2 patients, we collected n = 22 CSF samples at T0, and n = 17 at T302. For SMA3 patients, we collected n = 17 CSF samples at T0, and $n = 14$ CSF samples at T302 (Table 3). For longitudinal analysis, we considered the subgroup of SMA patients (n = 18 SMA1, n = 17 SMA2, and n = 14 SMA3) for whom CSF samples were available both prior to (T0) and 302 days after (T302) initiation of treatment, corresponding to the maintenance phase of Nusinersen therapy (Fig. 2A; Table 3). All patients were clinically diagnosed and genetically confirmed, and the *SMN2* copy number was also determined. All SMA1 patients, irrespective of age and disease severity, were part of the Expanded Access Programme (EAP) for compassionate use to patients with the infantile form only, which occurred in Italy between November 2016 and November 2017. Most of the patients included in this cohort had a long disease duration before starting Nusinersen therapy. The overall clinical response of these patients to Nusinersen treatment has previously been reported as part of the full Italian cohort and showed that therapeutic efficacy is related to age and clinical severity at baseline (Pane et al., 2019; Pane et al., 2018). The SMA2 and SMA3 patients have also been reported previously (Coratti et al., 2021).

4.2. Clinical evaluation

Assessment of patients was performed at T0 and T302. At each visit, extensive clinical examination was performed by experienced child neurologists or pediatricians with expertise in SMA, and anthropometric measurements and vital parameters were collected. Patients' feeding status (oral nutrition, nasogastric tube or percutaneous gastrostomy), nutritional status postulated by Body Mass Index (BMI), and respiratory function (spontaneous breathing, NIV or tracheostomy) were recorded.

For SMA1 patients, five children were younger than 5 months, while all the others were older than 5 months at the beginning of treatment, with ages ranging from 6 months to 10 years. Eleven patients had tracheostomy, and thirteen were under NIV for <16 h/day. Nineteen patients had gastrostomy, and the BMI fell into the underweight range (< 18.5) in all patients. The age of the SMA2 patients included in this study ranged from 9 months to 13.6 years at baseline. Seven of these patients were under NIV, and fourteen patients were in spontaneous breathing. None had tracheostomy or gastrostomy, and the BMI fell below 18 in eight patients. Regarding the SMA3 patients, one was under NIV for <16 h/day, and none had gastrostomy. At T0 and T302, all patients were assessed using standardized motor function tests chosen according to their age and motor function by trained physiotherapists. Functional assessments were performed by expert physiotherapists trained with standardized procedure manuals (Glanzman et al., 2018) and reliability sessions. SMA1 patients were assessed with the CHOP-INTEND (Glanzman et al., 2010; Glanzman et al., 2011), a functional scale including 16 items aimed at assessing motor function in weak infants. Each item is scored from 0 to 4 (0 being no response and 4 being the complete level of response), with a total score ranging from 0 to 64. SMA2 and SMA3 patients were evaluated with the HFMSE (Glanzman et al., 2011; O'Hagen et al., 2007), a scale of 33 items investigating the child's ability to perform different activities. The total score can range from zero, if all the activities are failed, to 66, indicating better motor function. All patients were not wearing spinal jackets or orthoses during the evaluations. SMA1, SMA2 and SMA3 patients significantly differed in age (SMA1 *vs* SMA2, $P = 0.006$; SMA1 *vs* SMA3, $P < 0.0001$; SMA2 *vs* SMA3, $P = 0.004$; Mann-Whitney test). BMI was lower in SMA1 compared to SMA2 and SMA3 patients ($P = 0.0001$ and $P = 0.002$, respectively; Mann-Whitney test) while sex was not different among SMA groups ($\chi^2 = 0.045$, $P = 0.978$).

4.3. Intrathecal treatment with Nusinersen

Intrathecal administration of 12 mg of Nusinersen was performed in a hospital environment. Fasting less than 4 h was planned for the procedure in SMA1 patients, while the time between the last meal and the lumbar puncture was 6–8 h in SMA2 and SMA3 patients. In SMA1 the procedure was carried out without sedation, whereas for SMA2 and SMA3 patients a sedation with midazolam was applied. No severe adverse events were reported. After the infusion, all patients were recommended to lie for 2 h to avoid any possible post-lumbar puncture symptoms.

4.4. CSF sample collection

CSF samples were collected at the time of intrathecal administration of Nusinersen in polypropylene tubes and stored at −80 °C until further analysis. Amino acid levels were measured in the CSF sample of each patient. Exclusion criteria included the presence of symptoms or changes in blood biochemical and haematological parameters suggestive of a systemic inflammatory state, and/or immunosuppressive treatments ongoing in the last 6 months before inclusion.

4.5. Animals

Experiments in mice were performed according to the international

guidelines for animal research and approved by the Animal Care Committee of "Federico II" University of Naples, Italy and the Ministry of Health, Italy. Heterozygous SMNΔ7 carrier mice ($Smn^{+/-}$; $SMN2^{+/+}$; $SMN\Delta7^{+/+}$) were purchased from Jackson Laboratory (stock number 005025) and bred to obtain $Smn^{+/+}$ (WT) animals and $Smn^{-/-}$ (SMA) animals. Mice were housed with 12 h light/dark cycle and were given free access to food and water. All efforts were made to minimize animal suffering and to reduce the number of animals used. The colony was maintained by interbreeding carrier mice, and the offspring were genotyped by PCR assays on tail DNA according to the protocols provided by Jackson Laboratory as previously reported (Valsecchi et al., 2020). Data were obtained from brain and spinal cord tissue of WT and SMNΔ7 mice isolated at P3 and P11, considering P0 as the day of birth.

4.6. HPLC detection

CSF samples (100 µL) were mixed in a 1:10 dilution with HPLC-grade methanol (900 µL) and centrifuged at 13,000 ×*g* for 10 min; supernatants were dried and then suspended in 0.2 M trichloroacetic acid (TCA). Mouse brain and spinal cord frozen samples were homogenized in 1:10 (*w/v*) 0.2 M TCA, sonicated (4 cycles, 10 s each), and centrifuged at 13,000 ×*g* for 20 min. TCA supernatants from mice and human samples were then neutralized with NaOH and subjected to pre-column derivatization with o-phthalaldehyde (OPA)/*N*-acetyl-L-cysteine (NAC). Diasteroisomer derivatives were resolved on a UHPLC Agilent 1290 Infinity (Agilent Technologies, Santa Clara, CA, USA) using a ZORBAX Eclipse Plus C8, 4.6 × 150 mm, 5 µm (Agilent Technologies, Santa Clara, CA, USA) under isocratic conditions (0.1 M sodium acetate buffer, pH 6.2, 1 % tetrahydrofuran, and 1.5 mL/min flow rate). A washing step in 0.1 M sodium acetate buffer, 3 % tetrahydrofuran, and 47 % acetonitrile was performed after every single run. Identification and quantification of D-Asp, L-Asp, L-Glu, D-Ser, L-Ser, and L-Gln were based on retention times and peak areas, compared with those associated with external standards. For quantification of each amino acid, a calibration curve of eight to fourteen points that covered the range of predicted analyte concentration in the test samples was generated using reference solutions. The R^2 value for each curve was at least 0.998 for CSF and 0.999 for mouse tissues. All the precipitated protein pellets from mice samples were solubilized in 1 % SDS solution and quantified by bicinchoninic acid (BCA) assay method (Pierce™ BCA Protein Assay Kits, Thermofisher Scientific, Rockford, IL, USA). The concentration of amino acids in tissue homogenates was normalized to the total protein content and expressed as nmol/mg protein. Amino acid levels in the CSF were expressed as micromolar (µM).

4.7. Drug treatment and behavioral assays in SMA mice

For studies of D-Ser supplementation in SMA mice, all procedures were performed on postnatal mice in accordance with the NIH guidelines and approved by the Institutional Laboratory Animal Care and Use Committee of Columbia University. FVB.Cg-*Grm7*$^{Tg(SMN2)89Ahmb}$ *Smn1*^{tm1Msd} Tg(SMN2*delta7)4299Ahmb/J (JAX Strain # 005025) mice were interbred to obtain SMA mutant mice (Le et al., 2005). Mice were housed in a 12 h/12 h light/dark cycle with access to food and water *ad libitum*. Mice from all experimental groups were monitored daily for weight, motor function, and survival from birth to 21 days of age. The righting reflex was assessed by placing the mouse on its back and measuring the time it took to turn upright on its four paws (righting time). The cut-off test time was 60 s. For each testing session, the test was repeated three times, and the mean of the recorded times was calculated. D-Ser (Sigma #S4250) was dissolved in water, filter sterilized and delivered daily at a dose of 500 mg/kg by intraperitoneal injections starting from P0. Approximately equal proportions of mice of both sexes were used, and aggregated data were presented because gender-specific differences were not found.

4.8. Protein analysis

For Western blot analysis, mice were euthanized and spinal cord collection was performed in a dissection chamber under continuous oxygenation (95 %O_2/5 %CO_2) in the presence of cold (~12 °C) artificial cerebrospinal fluid (aCSF) containing 128.35 mM NaCl, 4 mM KCl, 0.58 mM NaH_2PO_4, 21 mM $NaHCO_3$, 30 mM D-Glucose, 1.5 mM $CaCl_2$, and 1 mM $MgSO_4$. Total protein extracts were generated by homogenization of spinal cords in SDS sample buffer (2 % SDS, 10 % glycerol, 5 % ß-mercaptoethanol, 60 mM Tris-HCl pH 6.8, and bromophenol blue), followed by brief sonication and boiling. Proteins were quantified using the *RC DC*™ Protein Assay (Bio-Rad) and 25 µg of protein extract was analyzed by SDS/PAGE on 12 % polyacrylamide gels followed by Western blotting as previously described (Carlini et al., 2024). Anti-SMN mouse monoclonal antibody (BD Transd Lab, clone 8, #610646; 1:10,000), anti-GAPDH mouse monoclonal antibody (Sigma, clone 6C5, #MAB374, 1:50,000), and HRP conjugated goat anti-mouse secondary antibody (Jackson #115–035-044; 1:10,000) were used. The signal was detected using an iBrigth CL1500 Imaging System (Thermo Fisher Scientific) and image quantification was processed with the iBright Analysis Software (version 5.1.0).

4.9. Statistical analysis

Statistical analyses were performed using SPSS software v.27 (SPSS Inc., Chicago, IL, USA) and R Language v.4.3.2 (R Foundation for Statistical Computing, Vienna, Austria). Normality distribution was assessed by q-q plot and Shapiro–Wilk test. Quantitative variables were expressed by the median and interquartile range (IQR), while qualitative variables were by absolute or relative frequency. The correlation was evaluated by non-parametric Spearman's rho. The effect of confounders on correlation was evaluated by partial correlation and multivariate linear regression on natural log-transformed data. Differences between independent groups were studied by the non-parametric Kruskal-Wallis test followed, if statistically significant, by post-hoc tests performed by the Mann-Whitney test with Bonferroni's correction. The effect of confounders was evaluated by ANCOVA on natural log-transformed variables. Differences between dependent groups were studied by non-parametric Friedman test followed, if statistically significant, by post-hoc tests performed by Wilcoxon Signed Ranks Test with Bonferroni's correction. Amino acid concentrations in the CNS of SMA and WT mice were compared using Mann-Whitney test and two-way ANOVA followed by Tukey's *post-hoc* using Prism 8 version 8.0.2. For studies of D-Ser supplementation in SMA mice, statistical analysis of SMN protein levels was performed by one-way ANOVA with Šídák's multiple comparisons test. Differences in weight gain and motor function were analyzed by two-way ANOVA with Tukey's multiple comparison test. A comparison of survival curves was performed using the Log-rank (Mantel-Cox) test. Prism 10 for macOS version 10.3.1 was used for these statistical analyses.

Supplementary data to this article can be found online at https://doi.org/10.1016/j.nbd.2025.106849.

Funding sources

A.U., G.P., T.N., R.d.V., E.B., and A.D.A. were supported by #NEXTGENERATIONEU (NGEU) funded by the Ministry of University and Research (MUR), National Recovery and Resilience Plan (NRRP), project MNESYS (PE0000006) – A Multiscale integrated approach to the Study of the Nervous System in Health and Disease (DN. 1553 11.10.2022). E.B. and A.D.A. were also supported by a grant from Ricerca Finalizzata from the Italian Ministry of Health (Project nr RF-2019-12,370,334); E.B., A.D., C.P. and C.B. are members of the ERN NMD European Network (Project nr 2016/557). C.B. and F.E. were supported by Ministry of Health, NextGenerationEU (Project PNRR-POC-2023-12,377,653). L.P. was supported by NIH grants

R01NS102451, R01NS114218, and R01NS116400.

CRediT authorship contribution statement

Amber Hassan: Investigation, Visualization. **Raffaella di Vito:** Investigation, Formal analysis, Visualization. **Tommaso Nuzzo:** Visualization, Formal analysis. **Matteo Vidali:** Formal analysis. **Maria Jose Carlini:** Investigation, Formal analysis. **Shubhi Yadav:** Investigation, Formal analysis. **Hua Yang:** Investigation, Formal analysis. **Adele D'Amico:** Resources. **Xhesika Kolici:** Resources. **Valeria Valsecchi:** Resources. **Chiara Panicucci:** Resources. **Giuseppe Pignataro:** Resources. **Claudio Bruno:** Resources. **Enrico Bertini:** Resources. **Francesco Errico:** Writing – review & editing, Writing – original draft. **Livio Pellizzoni:** Writing – review & editing, Writing – original draft, Supervision, Funding acquisition. **Alessandro Usiello:** Writing – review & editing, Writing – original draft, Supervision, Project administration, Funding acquisition, Conceptualization.

Declaration of competing interest

C.B. received advisory board honoraria from Avexis, Biogen, Novartis and Roche. The other authors declare no competing interests.

Data availability

Data will be made available on request.

References

Abati, E., et al., 2020. Glial cells involvement in spinal muscular atrophy: could SMA be a neuroinflammatory disease?, 140, 104870.

Andersen, J.V., et al., 2021. Glutamate metabolism and recycling at the excitatory synapse in health and neurodegeneration. Neuropharmacology 196, 108719.

Biondi, O., et al., 2008. Exercise-induced activation of NMDA receptor promotes motor unit development and survival in a type 2 spinal muscular atrophy model mouse. J. Neurosci. 28, 953–962.

Biondi, O., et al., 2010. In vivo NMDA receptor activation accelerates motor unit maturation, protects spinal motor neurons, and enhances SMN2 gene expression in severe spinal muscular atrophy mice. J. Neurosci. 30, 11288–11299.

Bough, K.J., et al., 2007. Evidence against enhanced glutamate transport in the anticonvulsant mechanism of the ketogenic diet. Epilepsy Res. 74, 232–236.

Branchu, J., et al., 2013. Shift from extracellular signal-regulated kinase to AKT/cAMP response element-binding protein pathway increases survival-motor-neuron expression in spinal-muscular-atrophy-like mice and patient cells. J. Neurosci. 33, 4280–4294.

Buettner, J.M., et al., 2021. Central synaptopathy is the most conserved feature of motor circuit pathology across spinal muscular atrophy mouse models, p. 24.

Carlini, M.J., et al., 2024. Stasimon/Tmem41b is required for cell proliferation and adult mouse survival, 712, 149923.

Chaytow, H., et al., 2021. Spinal muscular atrophy: from approved therapies to future therapeutic targets for personalized medicine, p. 2.

Coratti, G., et al., 2021. Motor function in type 2 and 3 SMA patients treated with Nusinersen: a critical review and meta-analysis. Orphanet J. Rare Dis. 16, 430.

Coyle, J.T., et al., 2020. D-serine, the shape-shifting NMDA receptor co-agonist. Neurochem. Res. 45, 1344–1353.

Curtis, D.R., Watkins, J.C., 1960. The excitation and depression of spinal neurones by structurally related amino acids. J. Neurochem. 6, 117–141.

de Ceglia, R., et al., 2023. Specialized astrocytes mediate glutamatergic gliotransmission in the CNS, 622, pp. 120–129.

de Oliveira Souza, I.N., et al., 2023. D-amino acids: new clinical pathways for brain diseases.

Deguise, M.O., et al., 2021. Metabolic dysfunction in spinal muscular atrophy. Int. J. Mol. Sci. 22.

Delestrée, N., et al., 2023. Serotonergic dysfunction impairs locomotor coordination in spinal muscular atrophy. Brain 146, 4574–4593.

Di Maio, A., et al., 2023. Homeostasis of serine enantiomers is disrupted in the post-mortem caudate putamen and cerebrospinal fluid of living Parkinson's disease patients. Neurobiol. Dis. 184, 106203.

Dienel, G.A., 2013. Astrocytic energetics during excitatory neurotransmission: what are contributions of glutamate oxidation and glycolysis? Neurochem. Int. 63, 244–258.

Dingledine, R., et al., 1999. The glutamate receptor ion channels. Pharmacol. Rev. 51, 7–61.

Errico, F., et al., 2020. New insights on the influence of free d-aspartate metabolism in the mammalian brain during prenatal and postnatal life, 1868, 140471.

Errico, F., et al., 2022. Nusinersen induces disease-severity-specific neurometabolic effects in spinal muscular atrophy, 12, p. 1431.

Finkel, R.S., et al., 2017. Nusinersen versus sham control in infantile-onset spinal muscular atrophy, 377, pp. 1723–1732.

Fletcher, E.V., et al., 2017. Reduced sensory synaptic excitation impairs motor neuron function via Kv2.1 in spinal muscular atrophy. Nat. Neurosci. 20, 905–916.

Fletcher, E.V., et al., 2024. Synaptic imbalance and increased inhibition impair motor function in SMA. bioRxiv.

Fuchs, S.A., et al., 2006. D-serine in the developing human central nervous system. Ann. Neurol. 60, 476–480.

Garofalo, K., et al., 2011. Oral L-serine supplementation reduces production of neurotoxic deoxysphingolipids in mice and humans with hereditary sensory autonomic neuropathy type 1. J. Clin. Invest. 121, 4735–4745.

Glanzman, A.M., et al., 2010. The children's hospital of Philadelphia infant test of neuromuscular disorders (CHOP INTEND): test development and reliability. Neuromuscul. Disord. 20, 155–161.

Glanzman, A.M., et al., 2011. Validation of the children's hospital of Philadelphia infant test of neuromuscular disorders (CHOP INTEND). Pediatr. Phys. Ther. 23, 322–326.

Glanzman, A.M., et al., 2018. Evaluator training and reliability for SMA global Nusinersen Trials1. J. Neuromuscul. Dis. 5, 159–166.

Hamilton, G., Gillingwater, T.H., 2013. Spinal muscular atrophy: going beyond the motor neuron. Trends Mol. Med. 19, 40–50.

Hashimoto, K., et al., 2005. Reduced D-serine to total serine ratio in the cerebrospinal fluid of drug naive schizophrenic patients, 29, pp. 767–769.

Hashimoto, K., et al., 2009. Co-administration of a D-amino acid oxidase inhibitor potentiates the efficacy of D-serine in attenuating prepulse inhibition deficits after administration of dizocilpine. Biol. Psychiatry 65, 1103–1106.

Hernandez-Gerez, E., et al., 2020. Widespread tissue hypoxia dysregulates cell and metabolic pathways in SMA, 7, pp. 1580–1593.

Imarisio, A., et al., 2024a. Blood D-serine levels correlate with aging and dopaminergic treatment in Parkinson's disease. Neurobiol. Dis. 192, 106413.

Imarisio, A., et al., 2024b. Serum dysregulation of serine and glycine metabolism as predictive biomarker for cognitive decline in frail elderly subjects. Transl. Psychiatry 14, 281.

Imlach, W.L., et al., 2012. SMN is required for sensory-motor circuit function in Drosophila. Cell 151, 427–439.

Kong, L., et al., 2021. Impaired prenatal motor axon development necessitates early therapeutic intervention in severe SMA. Sci. Transl. Med. 13.

Le, T.T., et al., 2005. SMNΔ7, the major product of the centromeric survival motor neuron (SMN2) gene, extends survival in mice with spinal muscular atrophy and associates with full-length SMN, 14, pp. 845–857.

Lefebvre, S., et al., 1995. Identification and characterization of a spinal muscular atrophy-determining gene. Cell 80, 155–165.

Leo, M., et al., 2022. Induction of survival of motor neuron (SMN) protein deficiency in spinal astrocytes by small interfering RNA as an in vitro model of spinal muscular atrophy, 11, p. 558.

Levine, T.D., et al., 2017. Phase I clinical trial of safety of L-serine for ALS patients. In: Amyotroph Lateral Scler Frontotemporal Degener, 18, pp. 107–111.

Li, Y., et al., 2023. An overview of the therapeutic strategies for the treatment of spinal muscular atrophy, 34, pp. 180–191.

Ling, S., et al., 2010. Identification of the rheumatoid arthritis shared epitope binding site on calreticulin. PLoS One 5, e11703.

Liu, Z.-L., et al., 2023. Angiogenic signaling pathways and anti-angiogenic therapy for cancer, 8, p. 198.

Lotti, F., et al., 2012. An SMN-dependent U12 splicing event essential for motor circuit function. Cell 151, 440–454.

Malik, A.R., Willnow, T.E., 2019. Excitatory amino acid transporters in physiology and disorders of the central nervous system, 20, p. 5671.

Martin, J.E., et al., 2017. Decreased motor neuron support by SMA astrocytes due to diminished MCP1 secretion, 37, pp. 5309–5318.

Mayer, M.L., 2005. Glutamate receptor ion channels, 15, pp. 282–288.

Mayer, M.L., 2006. Glutamate receptors at atomic resolution, 440, pp. 456–462.

Meftah, A., et al., 2021. D-serine: a cross species review of safety. Front. Psychol. 12, 726365.

Mentis, G.Z., et al., 2011. Early functional impairment of sensory-motor connectivity in a mouse model of spinal muscular atrophy. Neuron 69, 453–467.

Mercuri, E., et al., 2020. Spinal muscular atrophy - insights and challenges in the treatment era. Nat. Rev. Neurol. 16, 706–715.

Mitchell, J., et al., 2010. Familial amyotrophic lateral sclerosis is associated with a mutation in D-amino acid oxidase, 107, pp. 7556–7561.

Molinaro, A.M., 2015. Diagnostic tests: how to estimate the positive predictive value, 2, pp. 162–166.

Morland, C., et al., 2013. Vesicular uptake and exocytosis of L-aspartate is independent of sialin, 27, p. 1264.

Murtas, G., et al., 2020. L-serine synthesis via the phosphorylated pathway in humans, 77, pp. 5131–5148.

Nilsson, M., et al., 1997. Glycine and D-serine decrease MK-801-induced hyperactivity in mice. J. Neural Transm. (Vienna) 104, 1195–1205.

Nishio, H., et al., 2023. Spinal muscular atrophy: the past, present, and future of diagnosis and treatment. Int. J. Mol. Sci. 24.

Nomura, J., et al., 2016. Role for neonatal D-serine signaling: prevention of physiological and behavioral deficits in adult Pick1 knockout mice. Mol. Psychiatry 21, 386–393.

Nuzzo, T., et al., 2023. Nusinersen mitigates neuroinflammation in severe spinal muscular atrophy patients. Commun. Med. (Lond). 3, 28.

O'Hagen, J.M., et al., 2007. An expanded version of the Hammersmith functional motor scale for SMA II and III patients. Neuromuscul. Disord. 17, 693–697.

Ohuchi, K., et al., 2019. Notch signaling mediates astrocyte abnormality in spinal muscular atrophy model systems, 9, p. 3701.

Orzylowski, M., et al., 2021. An overview of the involvement of D-serine in cognitive impairment in Normal aging and dementia. Front. Psychol. 12, 754032.
Pagiazitis, J.G., et al., 2025. Catecholaminergic dysfunction drives postural and locomotor deficits in a mouse model of spinal muscular atrophy. Cell Rep. 44, 115147.
Pane, M., et al., 2018. An observational study of functional abilities in infants, children, and adults with type 1 SMA. Neurology 91, e696–e703.
Pane, M., et al., 2019. Nusinersen in type 1 spinal muscular atrophy: twelve-month real-world data. Ann. Neurol. 86, 443–451.
Piubelli, L., et al., 2021. Serum D-serine levels are altered in early phases of Alzheimer's disease: towards a precocious biomarker. Transl. Psychiatry 11, 77.
Ravi, B., et al., 2021. Gene-targeting therapeutics for neurological disease: lessons learned from spinal muscular atrophy, 72, pp. 1–14.
Reilly, A., et al., 2023. Curing SMA: are we there yet?, 30, pp. 8–17.
Rindt, H., et al., 2015. Astrocytes influence the severity of spinal muscular atrophy, 24, pp. 4094–4102.
Sasabe, J., et al., 2007. d-Serine is a key determinant of glutamate toxicity in amyotrophic lateral sclerosis, 26, pp. 4149–4159.
Sasabe, M., et al., 2011. Phosphorylation of a mitotic kinesin-like protein and a MAPKKK by cyclin-dependent kinases (CDKs) is involved in the transition to cytokinesis in plants, 108, pp. 17844–17849.
Shababi, M., et al., 2014. Spinal muscular atrophy: a motor neuron disorder or a multi-organ disease? J. Anat. 224, 15–28.
Simon, C.M., et al., 2019. Stasimon contributes to the loss of sensory synapses and motor neuron death in a mouse model of spinal muscular atrophy, 29, pp. 3885–3901 (e5).
Simon, C.M., et al., 2021. Chronic pharmacological increase of neuronal activity improves sensory-motor dysfunction in spinal muscular atrophy mice. J. Neurosci. 41, 376–389.
Simon, C.M., et al., 2024. Dysfunction of proprioceptive sensory synapses is a pathogenic event and therapeutic target in mice and humans with spinal muscular atrophy. medRxiv.
Squire, L.R., Bayley, P.J., 2007. The neuroscience of remote memory. Curr. Opin. Neurobiol. 17, 185–196.
Tejero, A., et al., 2024. Effect of chronic maternal L-Glu intake during gestation and/or lactation on oxidative stress markers, AMPA Glu1 receptor and adenosine A1 signalling pathway from foetal and neonatal cerebellum, 20, pp. 181–192.
Tisdale, S., Pellizzoni, L., 2015. Disease mechanisms and therapeutic approaches in spinal muscular atrophy. J. Neurosci. 35, 8691–8700.
Traynelis, S.F., et al., 2010. Glutamate receptor ion channels: structure, regulation, and function. Pharmacol. Rev. 62, 405–496.
Valsecchi, V., et al., 2020. miR-206 reduces the severity of motor neuron degeneration in the facial nuclei of the brainstem in a mouse model of SMA, 28, pp. 1154–1166.
Valsecchi, V., et al., 2023. SMN deficiency perturbs monoamine neurotransmitter metabolism in spinal muscular atrophy, 6, p. 1155.
van der Crabben, S.N., et al., 2013. An update on serine deficiency disorders. J. Inherit. Metab. Dis. 36, 613–619.
Walter, L.M., et al., 2018. Interventions targeting glucocorticoid-Krüppel-like factor 15-branched-chain amino acid signaling improve disease phenotypes in spinal muscular atrophy mice, 31, pp. 226–242.
Welby, E., Ebert, A.D.J.G., 2023. Diminished motor neuron activity driven by abnormal astrocytic EAAT1 glutamate transporter activity in spinal muscular atrophy is not fully restored after lentiviral SMN delivery, 71, pp. 1311–1332.
Wirth, B.J.T.I.N., 2021. Spinal muscular atrophy: in the challenge lies a solution, 44, pp. 306–322.
Wirth, B., et al., 2020. Twenty-five years of spinal muscular atrophy research: from phenotype to genotype to therapy, and what comes next. Annu. Rev. Genomics Hum. Genet. 21, 231–261.
Wolosker, H., Radzishevsky, I.J.B.S.T., 2013. The serine shuttle between glia and neurons: implications for neurotransmission and neurodegeneration, 41, pp. 1546–1550.
Zilio, E., et al., 2022. Mitochondrial dysfunction in spinal muscular atrophy, 23, p. 10878.